CONF-810602--17



# SHORT-PULSE SHOCK INITIATION OF GRANULAR EXPLOSIVES*

Robert E. Setchell
Shock Wave and Explosives Physics
Division 5131
Sandia National Laboratories†
Albuquerque, New Mexico 87185

An experimental investigation has examined how different rates of unloading affect the release of chemical energy in a granular explosive experiencing transient shock compression. A compressed-gas gun was used to generate two types of short-pulse shocks in the explosive PBX-9404. A shock pressure of 3.2 GPa sustained for 0.37 μs was produced in both cases, but differences in flyer-plate properties resulted in different unloading histories. In one case the impact interface was rapidly unloaded by the initial release wave, while in the second case the unloading required multiple release waves over several microseconds. A VISAR system was used to observe the evolution of these two waves for distances up to 10 mm. The recorded waveforms showed that the unloading rates had a dominant effect on chemical energy release and growth towards detonation. This effect is important for considerations of critical impact criteria, and should provide a strong test for predictive shock-initiation models.

## INTRODUCTION

A short-duration shock wave is generated in an explosive sample during impact by a thin flyer plate or foil. An improved understanding of the resulting initiation process within the explosive is important for optimizing the design of detonator systems that utilize thin-flyer impact, and for assessing the response of explosives accidentally subjected to transient shock compressions. In a granular explosive, the initiation process resulting from transient shock loading are particularly complex. Numerous studies on heterogeneous explosives have established that shock-wave growth towards detonation depends on the formation of local regions of elevated thermal energy, or "hot spots", having temperatures much higher than the bulk temperatures expected from plane-shock compression. A number of hydrodynamic, plastic-work, and frictional mechanisms have been suggested as probable hot-spot sources. Ignition occurs within hot-spot material where sufficient thermal energy is generated and retained. If enough material is initially ignited, a progressive release of chemical energy will result in shock strengthening until detonation conditions are achieved. The dominant mechanism for the release of chemical energy, such as by thermal explosions at hot spots or by rapid grain-burning about hot-spot ignition sites, depends on both the initial heterogeneity of the explosive and the local strength of the propagating shock wave. Progress in understanding the complicated physical and chemical processes resulting from shock compression is being made in recent studies, as summarized in Refs. 1 and 2. In short-pulse shock initiation, these processes are subjected to a sudden release of the axial stress after some time interval. Depending on the strength and timing of the release wave, and on the size of the explosive material, the

*This work sponsored by the U.S. Department of Energy under Contract DE-AC04-DP00789.
†A U.S. Department of Energy facility.

## DISCLAIMER

growth-to-detonation process will be unaffected, or delayed, or prevented.

In recent years considerable attention has been given to the concept of a critical impact condition for achieving detonation. Thin-flyer impact experiments have examined how growth-to-detonation is delayed or prevented as flyer velocity and flyer thickness are reduced (3-8). Walker and Wasley (5) found that the threshold between initiation and non-initiation in several explosives correlated closely with the kinetic energy of the flyer plate. They proposed that the threshold for achieving detonation be expressed in terms of a critical energy per unit area transmitted to the explosive. This critical energy criterion is given by: $pu\tau$ = constant , where p is the shock pressure, and u the particle velocity produced by the transmitted shock, and $\tau$ is the time from impact when the axial stress is relieved at the impact interface. An equivalent expression is: $p^2\tau/\rho_o U$ = constant, where $\rho_o$ is the initial density and U the velocity of the transmitted shock. Since $\rho_o U$ varies slowly with shock pressure, the most common form for this criterion is: $p^2\tau$ = constant. These expressions assume that the shock-Hugoniot curves for the flyer-plate material and for the explosive are very close to each other, resulting in nearly complete stress unloading at time $\tau$.

Although useful critical-energy values have been determined experimentally over fairly broad ranges of shock pressure and duration (5-8), a basic physical understanding of the critical energy criterion has not been established. This difficulty is a consequence of the limited understanding of the basic processes of hot-spot formation and chemical energy release during sustained-shock initiation. Despite these limitations, several analytical models for a critical impact criterion have been proposed. Using a thermal explosion model for chemical energy release, Hayes (9) derived a detonation threshold condition in the form: $p^n\tau$ = constant, with n having values near 2. In this model the growth to detonation is assumed to fail if the axial stress at the impact interface is released prior to complete reaction. In apparent contradition, Howe et al.(10) compared thermal explosion times at particular shock pressures with shock durations necessary to initiate detonations, and concluded that a thermal explosion model could not reproduce existing critical-energy measurements. Ramsay (11) did not consider specific energy release mechanisms, but obtained detonation thresholds by simply assuming that failure would occur if a release wave overtook the transmitted shock prior to the distance to detonation expected for a sustained shock having the same initial pressure. On a more fundamental level, Roth (12) and Stresau and Kennedy (13) suggested that detonation thresholds are directly related to hot-spot formation processes. Particle velocity criteria, rather than shock pressure criteria, were proposed for threshold conditions based on possible hot-spot mechanisms.

In the near future, an improved understanding of critical impact conditions should result from current work on developing predictive analytical models for shock-initiation processes. In particular, models for granular explosives are under development which incorporate fairly detailed descriptions of mechanisms for hot-spot formation and for chemical energy release (1, 14, 15). As specific initiation mechanisms are more accurately described and evaluated, these models should be able to reproduce observed properties such as critical energy criteria. A more demanding test of the models will be their ability to reproduce actual waveforms observed during transition to detonation. Initial comparisons have been reported between predicted pressure histories and pressure records measured with manganin gauges for a 3 GPa, 0.33 μsec shock generated in the granular explosive PBX-9404 (1, 14).

The basic purpose of the present work is to provide new experimental data for evaluating predictive shock-initiation models. A specific purpose is to examine how different rates of unloading affect the release of chemical energy behind a short-duration shock wave. In the experiments, short-pulse shocks are generated in the explosive PBX-9404 by planar impact of either a thin flyer plate of fused silica or a thicker plate of sapphire. Different impact velocities are used to produce a shock pressure of 3.2 GPa sustained for 0.37 μsec in both cases. These values represent an imparted energy prior to stress release that is two-thirds of the accepted critical energy to achieve detonation in this explosive. Because of differences in shock impedances, release waves from the thin fused-silica flyers result in sudden unloading at the impact interface to an axial stress below 1.0 GPa, whereas release waves from the sapphire flyers result in gradual, stepped unloading requiring several microseconds. A double-delay laser interferometry system (VISAR) is used to observe how the waves corresponding to each of the impact conditions evolve over propagation

distances from 2 mm to 10 mm. A more detailed description of these experimental procedures is provided in the next section. Included in this section are calculated profiles for the initial waves in the explosive based on nominal impact conditions. The final sections present and discuss the observed behavior of these waves.

## EXPERIMENTAL PROCEDURES

The experiments were conducted using a compressed-gas gun capable of producing repeatable, planar impacts of projectiles 6.4 cm in diameter. A sketch of the experimental configuration is shown in Fig. 1. The fused silica and sapphire impactors were backed with 6.4 mm thick discs of 0.2 g/cm$^3$ carbon foam. The target assemblies consisted of a disc of PBX-9404 explosive followed by two discs of fused silica 1.6 mm and 12.7 mm thick. PBX-9404 was chosen for these experiments because of its extensive use in both experimental and analytical shock-initiation studies. The interface between the two fused silica pieces included a diffuse-reflecting layer of vacuum-deposited aluminum. A double-delay VISAR system (16) was used to measure particle velocity histories at this interface. The 1.6 mm thick "buffer" disc of fused silica was placed between the PBX-9404 and the VISAR measurement interface in order to smooth spatial non-uniformities in the wave transmitted from the granular explosive. The elastic properties of fused silica (17) were used in a method-of-characteristics calculation to find the corresponding one-dimensional waveform at the explosive/buffer interface. The measured velocities were also corrected for wave-generated, refractive-index changes in the 12.7 mm thick fused silica window (18).

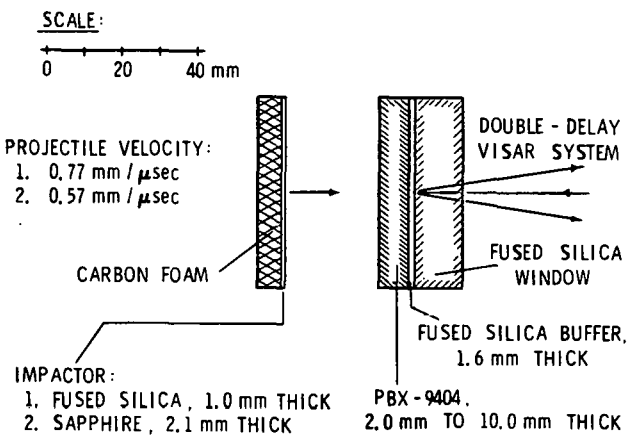


Fig. 1 Experimental configuration for short-pulse shock initiation studies.

Figure 2 shows a velocity history measured in a trial experiment designed to examine the wave motion generated in the sapphire impactor backed by carbon foam. The target for this experiment consisted of only a 9.6 mm thick disc of fused silica followed by a thicker fused silica window. The waveform shown in Fig. 2 was observed at the interface between these two fused silica pieces. An impact velocity of 0.353 km/sec was used in order to produce the same peak stress in the sapphire impactor as intended for the experiments with PBX-9404 targets. The finite risetime of the observed wave is a result of the unusual stress-strain behavior of fused silica below 4 GPa (17). The multiple release waves are a consequence of the impedance mismatch at the sapphire/fused silica impact interface. Also shown in Fig. 2 is a calculated waveform using the known properties of sapphire and fused silica, and assuming that no carbon foam was backing the sapphire impactor. The small differences between the measured and calculated profiles permit the carbon foam characteristics under shock loading to be identified. A waveform siliar to that shown in Fig. 2 was recorded in another trial experiment using a fused silica impactor. In this experiment the first release wave from the foam/impactor interface resulted in nearly complete stress unloading in the target.

similar

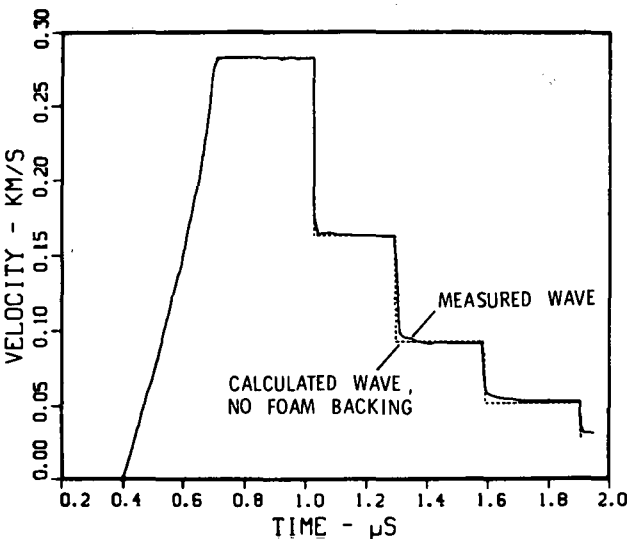


Fig. 2 Measured particle velocity history for a wave generated in fused silica by the impact of a thin sapphire disc backed by carbon foam. Dashed curve is a calculated waveform for this impact condition if the foam backing were absent.

Nominal impact velocities of 0.770 km/sec and 0.568 km/sec were used with the fused silica and sapphire impactors, respectively, in experiments with explosive targets. Impact velocities were repeatable to within 0.9%. With the fused silica and sapphire impactors having thicknesses of 1.02 mm and 2.05 mm, respectively, these impact conditions resulted in initial shock waves transmitted into the PBX-9404 samples having a peak axial stress of 3.2 GPa sustained for 0.37 μsec. Using the properties of fused silica, sapphire, and carbon foam, and a polynomial stress-strain fit to available shock-Hugoniot data for unreacted PBX-9404 (2), the unloading history at the impactor/explosive interface can be determined. Fig. 3 shows the calculated wave forms for the initial waves entering the PBX-9404 samples, assuming that no chemical reaction occurs. Since the shock Hugoniot for fused silica is much closer to the PBX-9404 Hugoniot than that for sapphire, the wave corresponding to the fused silica impactor shows much more rapid unloading.

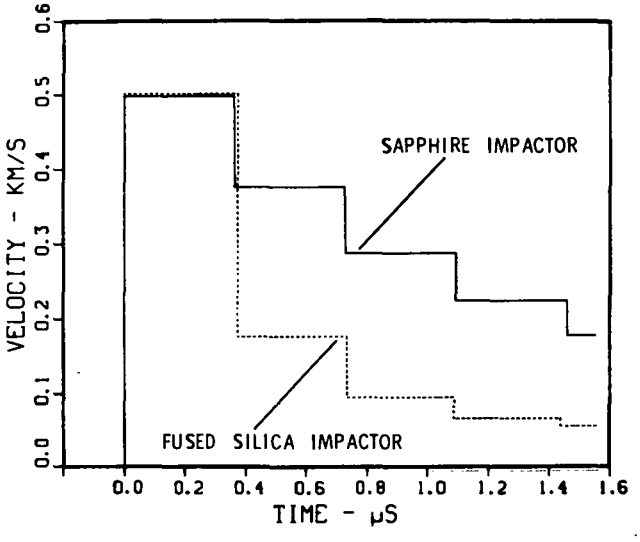


Fig. 3 Calculated initial waves into PBX-9404 generated by the impact of thin fused silica and sapphire discs.

An additional representation of the wave motion in the PBX-9404 targets is given by a distance-time diagram in Fig. 4. This diagram corresponds to the case of fused silica impact at 0.770 km/sec. The wave trajectories shown in PBX-9404 were calculated assuming that no chemical reactions occur, and that the polynomial stress-strain fit to Hugoniot data could be used to represent the material isentrope. With these assumptions, the initial rarefaction is seen to overtake the transmitted shock at a distance of 6.7 mm into the explosive. Also shown in Fig. 4 is a predicted particle path for material initially 2.0 mm into the explosive. At this position these inert-material calculations show the peak stress following shock arrival being sustained for only 0.26 μsec.

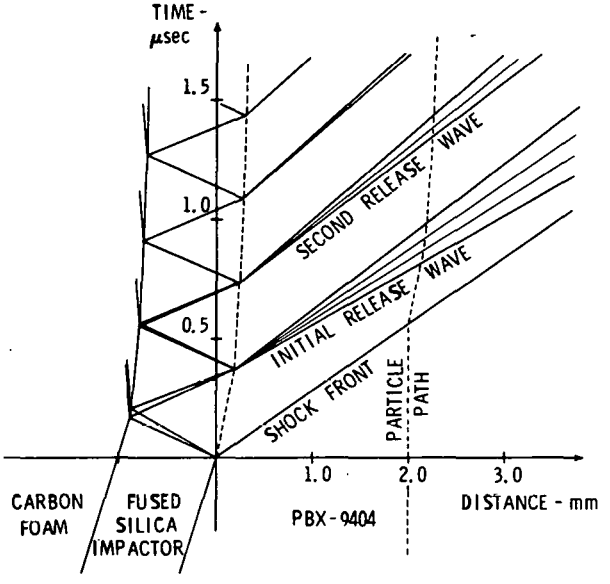


Fig. 4 Distance-time diagram for the waves generated by the impact of a thin fused silica disc onto PBX-9404. The explosive is assumed to be non-reactive, with an isentrope given by a fit to shock-Hugoniot data.

## RECORDED WAVEFORMS

The double-delay VISAR system provides two independent sets of fringe signals in which different fringe displacements result from a given change in particle velocity (16). A simultaneous reduction of the two sets of data eliminates possible uncertainties in reproducing velocity jumps due to shocks or rapid release waves. In all of the experiments the velocity histories determined from the two sets of fringe signals agreed to within 2%, consistent with the results of earlier calibration experiments using well-characterized target materials (Fig. 2). The VISAR signals were recorded for at least 3 μs following the wavefront in order to observe any evidence of chemical energy release occuring behind the wave. In the experiments using a sapphire impactor with the two

thickest discs of PBX-9404, however, the useful data recording time was reduced due to a loss in contrast in the VISAR signals. This difficulty resulted from the fused silica target discs being stressed beyond a phase transformation at approximately 9.4 GPa (2).

Figure 5 shows the particle velocity history recorded after wave propagation through 2.0 mm of PBX-9404 for an experiment using a fused silica impactor. This profile is the transmitted wave in fused silica at the explosive/buffer interface. Also shown in this figure is an "initial wave" in fused silica obtained from the predicted initial wave in the explosive (Fig. 3) using an approximate impedance-matching calculation. For this calculation the initial waveform in the explosive was assumed to be an established wave in inert material arriving at an interface with fused silica, and interactions between the multiple rarefactions in this incident wave and the waves reflected from the interface were included. In comparison, the measured waveform shows a slight increase in shock strength and a gradual increase in particle velocity prior to the arrival of the first release wave. This wave arrives approximately 0.14 μs after the shock front, which is much sooner than predicted by the inert-material calculations shown in Fig. 4. Except for the slight growth behind the shock front, the recorded waveform does not show any evidence of chemical energy release. Such evidence would appear as increases in measured velocities corresponding to compressive waves being generated downstream.

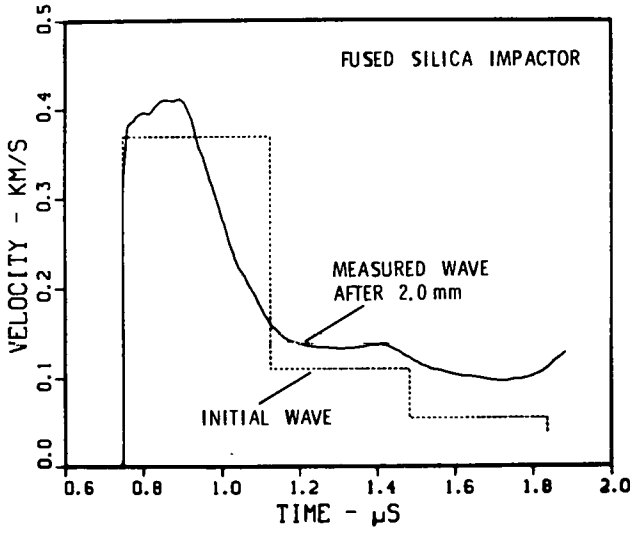


Fig. 5 Particle velocity history measured after wave propagation through 2.0 mm of PBX-9404, following impact by a thin fused silica disc. The recorded waveform is the transmitted wave in the fused silica buffer at the explosive/buffer interface. The dashed curve is a calculation showing the waveform prior to propagation through the explosive.

Figure 6 shows the velocity history recorded after 2.0 mm of explosive for an experiment using a sapphire impactor. A calculated "initial wave" in the fused silica buffer is also shown. The measured waveform shows a slightly greater increase in shock strength and a faster initial rise in velocity than observed with the fused silica impactor. The initial release wave again arrives approximately 0.14 μs after the shock front. Unlike the fused silica case, the waveform in Fig. 6 shows distinct compressive waves developing downstream of the shock front due to chemical energy release. The second rarefaction in the initial wave appears to be affecting the development of the downstream waves, but the subsequent rarefactions are not evident. These observations are not the result of waves reflected first from the buffer interface and then from the impactor, as conservative estimates for these interactions give longer arrival times than shown in the figure.

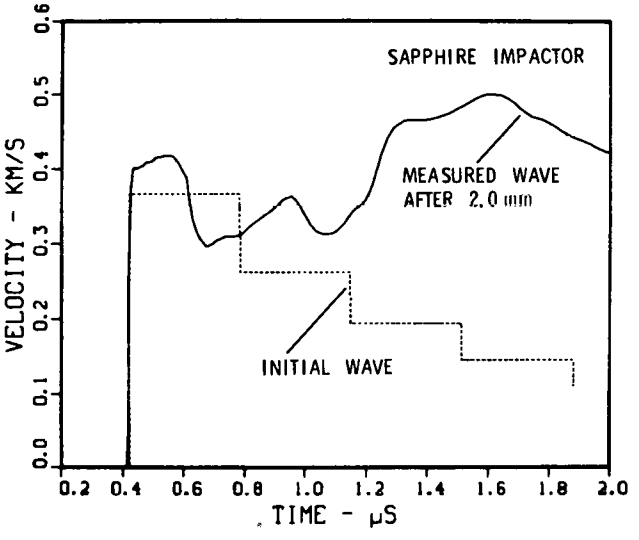


Fig. 6 Particle velocity history measured after 2.0 mm of PBX-9404, following impact by a thin sapphire disc. The dashed curve is the calculated waveform prior to propagation through the explosive.

Figures 7 and 8 present all of the velocity histories recorded for experiments using fused silica impactors. The individual records have been shifted in time to facilitate comparisons. In Fig. 7 the waveforms are displayed on an expanded time scale in order to show the evolution of the shock front. The first release wave overtakes the shock by 4.0 mm, again indicating sound speeds much higher than estimated by inert-material calculations (Fig. 4). The strength of the shock progressively decays after the arrival of this release wave, with the shock amplitude after 10.0 mm less than half that of the initial wave. On this time scale, the particle velocity following the first release wave appears to remain fairly constant with propagation distance. In Fig. 8, however, the entire velocity histories recorded after 4.0, 6.0, and 10.0 mm show a compressive disturbance being generated by chemical energy release at some distance behind the shock front. Although this disturbance is growing in amplitude, it does not appear to be rapidly overtaking the shock.

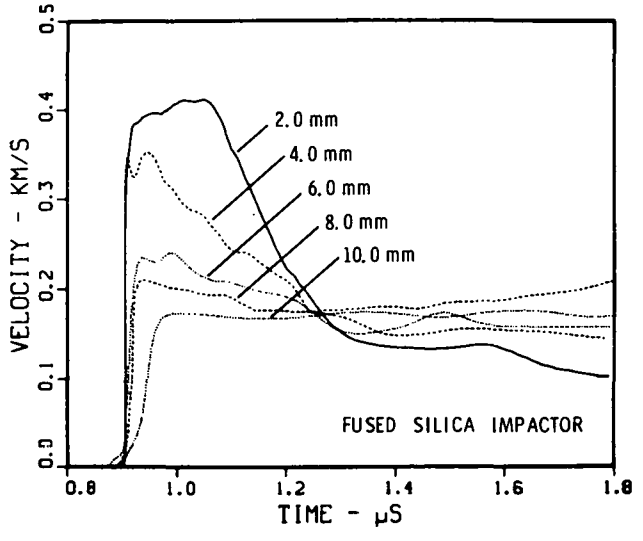


Fig. 7 Shock front evolution in the PBX-9404 experiments using fused silica impactors. The waveforms have been shifted in time to facilitate comparisons.

Figures 9 and 10 present the complete set of velocity histories recorded in experiments using sapphire impactors. These records are also shifted in time to permit direct comparisons. The evolution of the shock front is displayed on an expanded time scale in Fig. 9. The strength of the shock increases slightly until the front is overtaken by the first release wave,

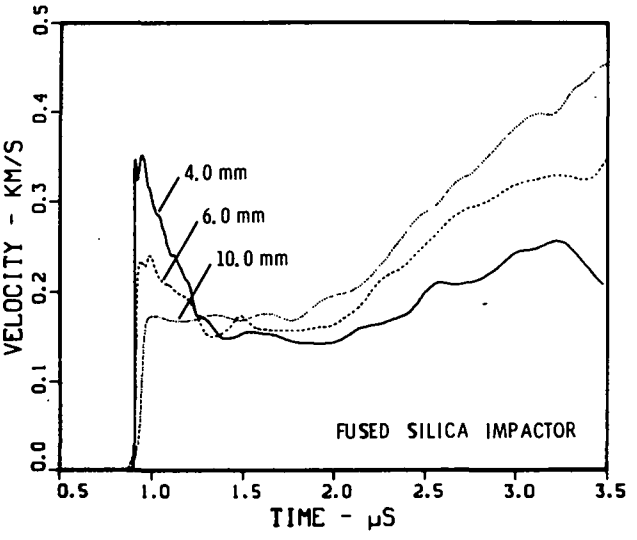


Fig. 8 Chemical energy release in the PBX-9404 experiments using fused silica impactors.

after which the strength decays. By 8.0 mm, however, the shock amplitude has increased suddenly due to the arrival of compressive waves generated downstream. The growth of these waves is displayed more fully in Fig. 10. Progressive chemical energy release is evident as the compressive disturbances grow and overtake the shock. This wave was not observed at distances greater than 8.0 mm, since the waveforms indicated that transition to detonation would occur shortly after the predicted run distance of 9 mm for a 3.2 GPa sustained shock.

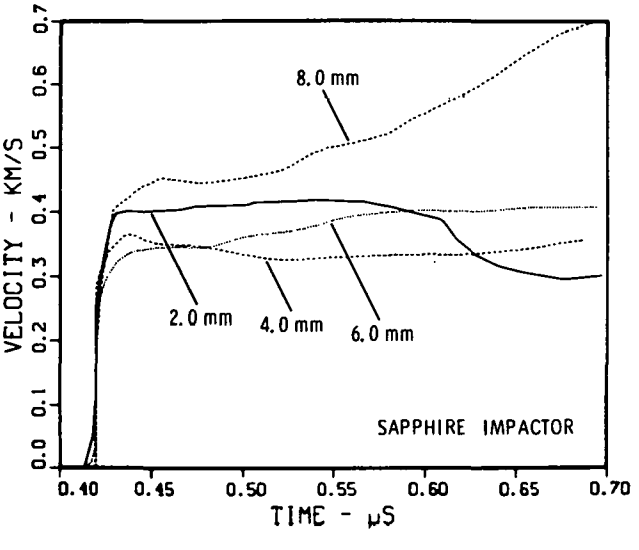


Fig. 9 Shock front evolution the PBX-9404 experiments using sapphire impactors.

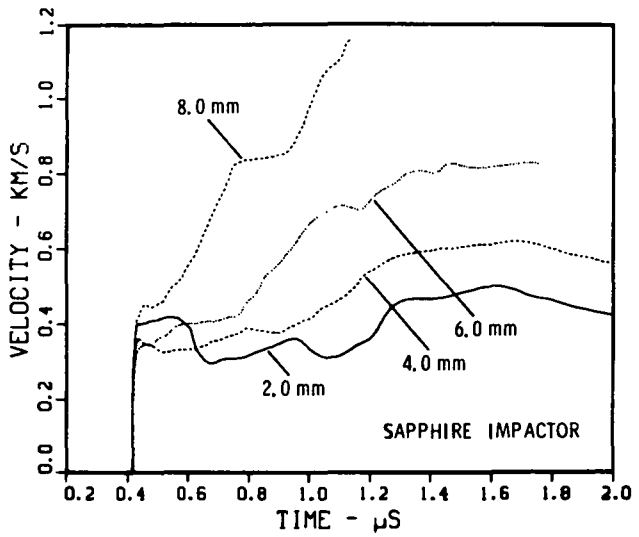


Fig. 10 Chemical energy release and wave growth in the PBX-9404 experiments using sapphire impactors.

## DISCUSSION

The basic goal of the present study was to obtain new data for the evaluation of predictive shock-initiation models. More specifically, the experiments examined how the rate of unloading affects energy release and growth towards detonation in the case of transient shock compression. The current VISAR measurements appear to be quite successful in meeting these objectives, for the two initial wave conditions having different unloading histories displayed fundamentally different behavior. The rapidly unloaded wave shows evidence of chemical energy release at some distance behind the wave front, but the resulting compressive disturbances do not appear to be rapidly overtaking the shock. Transition to detonation may still be possible, but a run distance much more than 10 mm would certainly be required. In sharp contrast, the slowly unloaded wave shows strong energy release downstream of the wavefront, with the resulting compressive disturbances rapidly overtaking and amplifying the shock. The final waveform recorded after 8.0 mm indicates that transition to detonation would occur shortly after the predicted sustained-shock run distance of 9 mm.

The observed differences in the evolution of the two initial waves suggest that some caution is necessary in utilizing critical impact criteria. Since the unloading history clearly affects the wave growth, comparisons or predictions based on $P^2\tau$ or $p_{ur}\tau$ criteria must consider if the particular flyer/explosive combination produces an initial release wave that results in nearly complete unloading. Unless the impedance match between the flyer material and the explosive is sufficiently close, a value of $p_{ur}\tau$ based on the initial shock amplitude and duration will not represent the total energy imparted into the explosive. Experiments to establish a critical energy criterion in PBX-9404 (4-6) have typically used aluminum impactors, for which the first release wave is slightly less effective for unloading the explosive than with fused silica impactors. Recent PBX-9404 short-pulse experiments used for initial comparisons with predictive models (1,14) were conducted with copper impactors, for which the first release wave unloads the explosive only slightly more than would a sapphire impactor. Although a basic physical understanding of critical impact criteria remains to be established, the present results support the integration of $p^2$ over the wave duration as a means of comparing non-square shock pulses with available $p^2\tau$ thresholds. Using the initial profiles shown in Fig. 3, this integration results in a value greater than the reported $p^2\tau$ threshold in PBX-9404 for the sapphire experiments, but a value less than this threshold for the fused silica experiments.

Finally, the recorded waveforms should provide a difficult test for predictive shock-initiation models in PBX-9404. Since the rate of unloading has a strong effect on chemical energy release, comparing model predictions with the present results should be particularly useful in evaluating different formulations for energy release mechanisms. More generally, the concept of experimentally isolating the effects of unloading rates on wave growth appears to be a productive addition to the methods available for studying shock initiation processes.

## ACKNOWLEDGEMENTS

The author would like to thank Mr. Joe A. Guzman for skillfully preparing and conducting the gas-gun experiments. Drs. L. W. Davison, J. E. Kennedy, J. W. Nunziato, and J. Wackerle contributed useful discussions during the course of this study.

## REFERENCES

1. E. L. Lee and C. M. Tarver, "Phenomenological Model of Shock Initiation in Heterogeneous Explosives", Phys. Fluids 23, 2362, (1980).

2. R. E. Setchell, "Ramp-Wave Initiation of Granular Explosives", Comb. Flame (in press).

3. E. F. Gittings, "Initiation of a Solid Explosive by a Short-Duration Shock", in Fourth Symp. (Int.) on Detonation, Office of Naval Research Rept. ACR-126 (1965), p.373.

4. B. D. Trott and R. G. Jung, "Effect of Pulse Duration on the Impact Sensitivity of Solid Explosives", in Fifth Symp. (Int.) on Detonation, Office of Naval Reserach Rept. ACR-184 (1970), p. 191.

5. F. E. Walker and R. J. Wasley, "Critical Energy for Shock Initiation of Heterogeneous Explosives", Explosivstoffe 1, 9 (1969).

6. D. E. Christiansen and J. W. Taylor, "HE Sensitivity Study", Los Alamos Scientific Laboratory Rept. LA-5440-MS (1973).

7. Y. de Longueville, C. Fauquignon and H. Moulard, "Initiation of Several Condensed Explosives by a Given Duration Shock Wave", in Sixth Symp. (Int.) on Detonation, Office of Naval Research Rept. ACR-221 (1976), p.105.

8. B. C. Taylor and L. H. Ervin, "Separation of Ignition and Buildup to Detonation in Pressed TNT", in Sixth Symp. (Int.) on Detonation, Office of Naval Research Rept. ACR-221 (1976), p. 3.

9. D. B. Hayes, "A $P^n t$ Detonation Criterion from Thermal Explosion Theory", in Sixth Symp. (Int.) on Detonation, Office of Naval Reserach Rept. ACR-221 (1976), p. 76.

10. P. Howe, R. Frey, B. Taylor and V. Boyle, "Shock Initiation and the Critical Energy Concept", in Sixth Symp. (Int.) on Detonation, Office of Naval Research Rept. ACR-221 (1976), p. 11.

11. J. B. Ramsay, "Short-Duration Shock-Wave Initiation of Solid Explosives", Acta. Astronautica 6, 771 (1979).

12. J. Roth, "Shock Sensitivity and Shock Hugoniots of High-Density Granular Explosives", in Fifth Symp . (Int.) on Detonation, Office of Naval Research Rept. ACR-184 (1970), p. 219.

13. R. H. Stresau and J. E. Kennedy, "Critical Conditions for Shock Initiation of Detonation in Real Systems", in Sixth Symp. (Int.) on Detonation, Office of Naval Research Rept. ACR-221 (1976), p. 68.

14. J. Wackerle, R. L. Rabie, M. J. Ginsberg and A. B. Anderson, "A Shock Initiation Study of PBX-9404", in Symp. (Int.) on High Dynamic Pressures, Commissariat a l'Energie Atomique, Paris (1978), p. 127.

15. E. K. Walsh, R. E. Setchell, M. E. Kipp and J. W. Nunziato, "Hot Spot Initiation of Heterogeneous Explosives", in Seventh Symp. (Int.) on Detonation.

16. A system similar in optical design is described in: R. A. Lederer, S. A. Sheffield, A. C. Schwarz and D. B. Hayes, "The Use of a Dual-Delay-Leg Velocity Interferometer with Automatic Data Reduction in a High-Explosive Facility", in Sixth Symp. (Int.) on Detonation, Office of Naval Research Rept. ACR-221 (1976), p. 210.

17. L. M. Barker and R. E. Hollenbach, "Shock-Wave Studies of PMMA, Fused Silica, and Sapphire", J. Appl. Phys. 41, 4208 (1970).

18. R. E. Setchell, "Index of Refraction of Shock-Compressed Fused Silica and Sapphire", J. Appl. Phys. 50, 8186 (1979).